LATE CARBONIFEROUS AGE CONFIRMED FOR THE OCEANIC PLATE OF PANTHALASSA PRESERVED IN THE KADOMA UNIT OF THE JURASSIC ACCRETIONARY COMPLEX IN NORTHEAST JAPAN

Shun Muto*,✉, **Tsuyoshi Ito*** and **Masanori Ozeki****

* *Geological Survey of Japan, AIST, Tsukuba, Japan.*
** *Graduate School of Life and Environmental Sciences, University of Tsukuba, Japan.*
✉ *Corresponding author, email: s-muto@aist.go.jp*

Keywords: *basalt; Carboniferous; chert; conodont; Kungurian; Moscovian; North Kitakami-Oshima Belt; Permian; radiolaria; Roadian; Sakmarian.*

ABSTRACT

Accretionary complexes in the Japanese Islands preserve material from parts of the oceanic plates of Panthalassa that have subducted and are now lost. The age of the oceanic plate that is incorporated into the Jurassic accretionary complex of Japan has been previously estimated from scant data on Carboniferous bedded chert. In this study, we investigated a Carboniferous to Permian basalt-chert sequence in the Jurassic accretionary complex of the North Kitakami-Oshima belt in Northeast Japan. The sequence is composed of basaltic rocks, red bedded chert and grey bedded chert in ascending order. The basaltic rocks at the base contain red cherty nodules that yielded conodonts indicating the Bashkiran to early Moscovian, the latter age being more likely (late Carboniferous). The red bedded chert yielded middle Sakmarian (early Permian) radiolarians. The grey bedded chert yielded conodonts indicating the latest Kungurian to earliest Roadian. Thus, our study section demonstrates a formation of the oceanic plate in the late Carboniferous and a following deposition of pelagic siliceous sediments. This is the first time that basaltic rocks within the Jurassic accretionary complex of Japan are directly dated. While previous data need careful reviewing, our results demonstrate that the oldest part of the oceanic plate within the Jurassic accretionary complex is Serpukhovian or older and the youngest part may be as young as the Sakmarian.

INTRODUCTION

The Jurassic accretionary complex in Japan is one of the most intensely studied accretionary complex formed in the Mesozoic (Kojima et al., 2016). It preserves records of the Superocean Panthalassa, which is a palaeogeographically significant realm due to its vastness (Fig. 1a). Despite this, the age of the oceanic plate in the Jurassic accretionary complex of Japan is largely enigmatic. While widely referenced works have stated that the basaltic rocks at the base of the oceanic plate stratigraphy in the Jurassic accretionary complex is Carboniferous (e.g., Isozaki et al., 1990; Wakita and Metcalfe, 2005), this is supported only from scant age data of Carboniferous chert (Ishiga, 1982; Imoto et al., 1997; Kusunoki et al., 2004). In other words, the basaltic rocks themselves have not actually been dated. Furthermore, the above consideration did not take into account any spatial variations due to poor availability of data. Recently, Ito and Matsuoka (2018) proposed that oceanic plate of a much younger age are present within the Jurassic accretionary complex of Japan. They showed that red bedded chert overlying basaltic rocks in Mt. Ryokami in the Kanto District is Sakmarian (early Permian) in age, coincident with the oldest cherts in many other localities.

In order to clarify the age of the oceanic plate that formed the Jurassic accretionary complex in Japan, it is necessary to obtain further age data from the lower part of the oceanic plate stratigraphy. In particular, age data from basaltic rocks, although never reported from the Jurassic accretionary complex, will give unambiguous informations. Works in other geological units, such as the Carboniferous accretionary complex in Northeast Japan (Hamano et al., 2002) have shown that microfossils can be obtained from cherty deposits within basaltic rocks (i.e., jasper).

Herein, we report conodonts and radiolarians from a sequence of basaltic rocks and chert exposed around the Hayasaka Highland in Iwate Prefecture (Figs. 1b, c, 2). The studied rocks belong to the Jurassic accretionary complex of the North Kitakami-Oshima Belt in Northeast Japan (Fig. 1c; Isozaki and Maruyama, 1991; Ehiro et al., 2008; Kojima et al., 2016). We conducted a geological mapping to clarify the mode of occurrence of the studied rocks and obtained age diagnostic microfossils to determine the age of the rocks.

GEOLOGICAL SETTING

Previous studies

The North Kitakami-Oshima Belt is the geotectonic division of Northeast Japan defined by the distribution of Jurassic accretionary complexes and spreads from northeast Tohoku to southwest Hokkaido (Fig. 1b, c; Isozaki and Maruyama, 1991; Ehiro et al., 2008; Kojima et al., 2016). The Jurassic accretionary complex is composed of basaltic rocks, bedded chert and palaeo-atoll limestone formed in the pelagic region, in addition to hemipelagic siliceous mudstone and tuff, mudstone and sandstone that accumulated near the trench (Ehiro et al., 2008). The accretionary complexes are intruded and thermally affected by Cretaceous plutons (Fig. 1c), which hinder extraction and identification of microfossils from both the oceanic and terrigenous rocks (Ehiro et al., 2008). Nonetheless, tenacious attempts by microfossil researchers revealed that the age of chert and limestone ranges from the Middle Pennsylvanian (late Carboniferous) to Middle Jurassic (see review by Uchino and Suzuki, 2020). The oldest ages are known from palaeo-atoll limestone in Ichinohe that was dated as somewhere within the Bashkirian to Kasimovian (probably Moscovian) (Ehiro et al., 2010) and dolostone

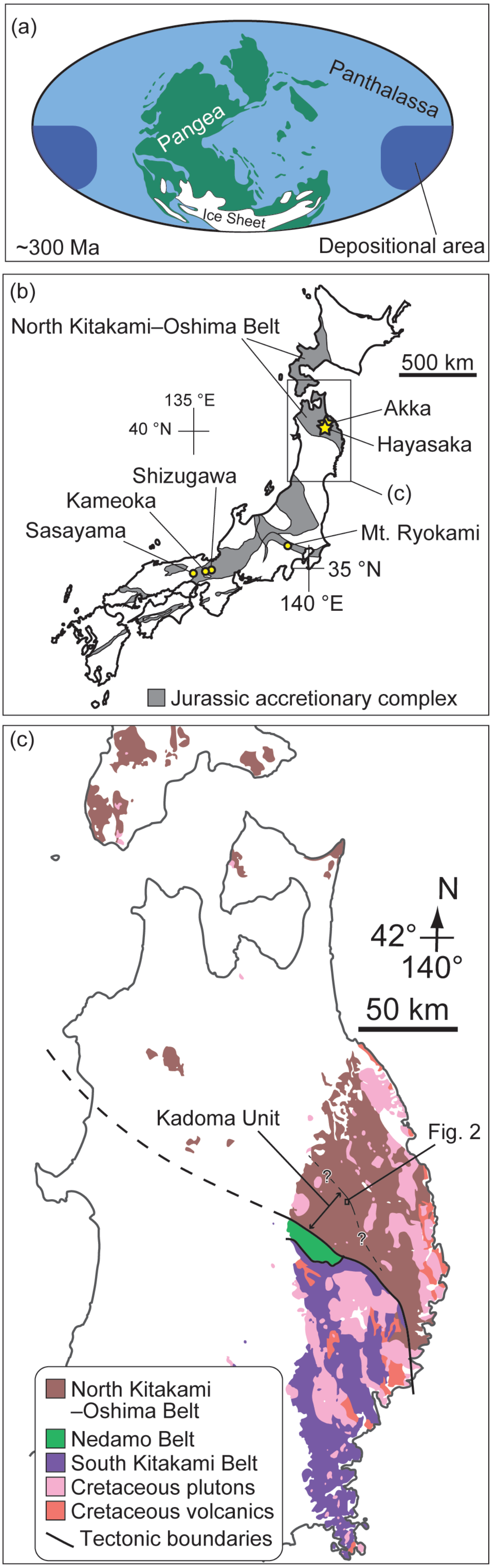

interbedded with chert in Okoshi Stream, Akka dated as Moscovian (Ehiro et al., 2008; Muto et al., 2023b). The age of accretion has also been investigated with microfossils, and, recently, by U-Pb dating of zircons in sandstone and tuff (Minoura and Tsushima, 1984; Matsuoka, 1987; 1988; Matsuoka and Oji, 1990; Yoshihara et al., 2002; Nakae and Kamada, 2003; Suzuki and Ogane, 2004; Suzuki et al., 2007a; 2007b; Ueda et al., 2009; 2018; Uchino, 2017; 2018a; 2018b; 2019; 2021a; Muto et al., 2023a; Osaka et al., 2023). These studies showed that the age of accretion is latest Triassic to earliest Cretaceous, with a general younging trend from southwest to northeast, i.e., towards the ocean.

The Hayasaka Highland is situated in the southwestern part of the NW-SE-trending Jurassic accretionary complex of the North Kitakami-Oshima Belt (Fig. 1c). Maps of 1:200,000 (Onuki 1981; Yoshida et al., 1984) and 1:100,000 (Iwate Prefecture, 1954) including the area have been published. However, they were produced before the concept of accretionary complexes were adopted and therefore many aspects of the geology is misinterpreted. Recently, a 1:50,000 geological map of the Sotoyama District, an area to the southwest of the Hayasaka Highland, was published, in which the accretionary complex including the rocks of the study area was referred to as the Kadoma Unit (Uchino, 2024). Previously, the Jurassic accretionary complex around the Hayasaka Highland was referred to as the Nakatsugawa Complex (Uchino et al., 2008; Osaka et al., 2023). However, this accretionary complex had been named the Kadoma Complex in the neighbouring area (Kawamura et al., 2013), prompting a revision of the name by Uchino (2024). Furthermore, following Uchino (2024), we use the term “unit” instead of “complex”, for tectonostratigraphic division of accretionary complexes, because the latter is not recommended where mappable rock bodies are present within or in case of coherent facies (Salvador, 2013).

The Kadoma Unit lies in the southwesternmost part of the Jurassic accretionary complex of the North Kitakami-Oshima Belt (Fig. 1c; Uchino, 2024). The accretionary age of the Kadoma Unit is estimated to be latest Triassic to Middle Jurassic (Matsuoka, 1988; Uchino, 2019; 2021a; Uchino and Suzuki, 2021; Osaka et al., 2023). Basaltic rocks of the Kadoma Unit include both mid-ocean ridge basalt (MORB) and ocean island basalt (OIB) (Uchino, 2021b). The basaltic rocks of the Hayasaka Highland, however, have not been investigated. Existing geological maps do not provide sufficient information on the geological background of the Hayasaka Highland due to the large scales of the maps and interpretations that do not consider subduction-accretion.

New data

We produced a geological map of the Hayasaka Highland as part of the survey for the 1:50,000 geological map of the Kado District for the Quadrangle Series of the Geological Survey of Japan (Fig. 2). The Kadoma Unit in this area is com-

Fig. 1 - (a) Palaeogeographic map by Mei and Henderson (2001) based on Ziegler et al. (1997). The depositional area of pelagic deep-sea sedimentary rocks preserved within Jurassic accretionary complexes of Japan is shown. (b) Distribution of the Jurassic accretionary complex in the Japanese Islands in the basement rocks (based on Isozaki et al., 2010) and previously studied localities mentioned in the text. (c) Exposure of pre-Paleogene rocks in northern Tohoku of Northeast Japan (modified from Geological Survey of Japan, AIST, 2020). The reader is referred to the PDF online for a colour version.

posed of muddy mixed rocks with bodies of basaltic rocks, chert, siliceous mudstone and sandstone. Bodies of basaltic rocks are up to 600 m thick, and are composed of massive to moderately foliated lava (Fig. 3a) and strongly foliated tuff (Fig. 3b). Bodies of chert are up to 100 m thick and are red or grey (Fig. 3c-f). Outcrops of red chert were only found around the junction of the Matsuzaki and Nekosokomatasawa rivers, but floats were found in other locations such as upstream along the Matsuzaki River. Siliceous mudstone occurs as bodies up to 200 m-thick, but mappable bodies are rare. Sandstone bodies are up to 200 m-thick, and are mostly massive (Fig. 3g). The muddy mixed rock that constitutes the majority of the Kadoma Unit in this area contains bodies of the above lithology within a muddy matrix. The muddy matrix includes variously deformed light-coloured silt, sand and tuff (Fig. 3h) and is consistent with the lithofacies referred to as "laminated mudstone" by Uchino (2021a). In addition to the above, we found mixed rocks with abundant light green claystone, possibly tuff within the muddy matrix, which are in fault contact with the Kadoma Unit to the east. This newly identified unit is not named in this study. The orientation of bedding and cleavage planes in the Kadoma Unit strike NNW-SSE to NW-SE and generally dip moderately to steeply to the west, but narrow zones of east dipping strata occur due to tight folds (Fig. 2).

We focused on a section of basaltic rocks and chert in the lowermost part of the Nekosokomatasawa River (Fig. 4). This section is observed along the stream itself and along the logging road on its north bank. For convenience, the rocks of the section are divided into four informal units. These are, in ascending order, basalt, lower red chert, upper red chert and grey chert units (Fig. 5). The stratigraphic order of these units was determined from microfossil occurrences or speculated from the overall geological structure, as explained below and in the following discussion on microfossil age.

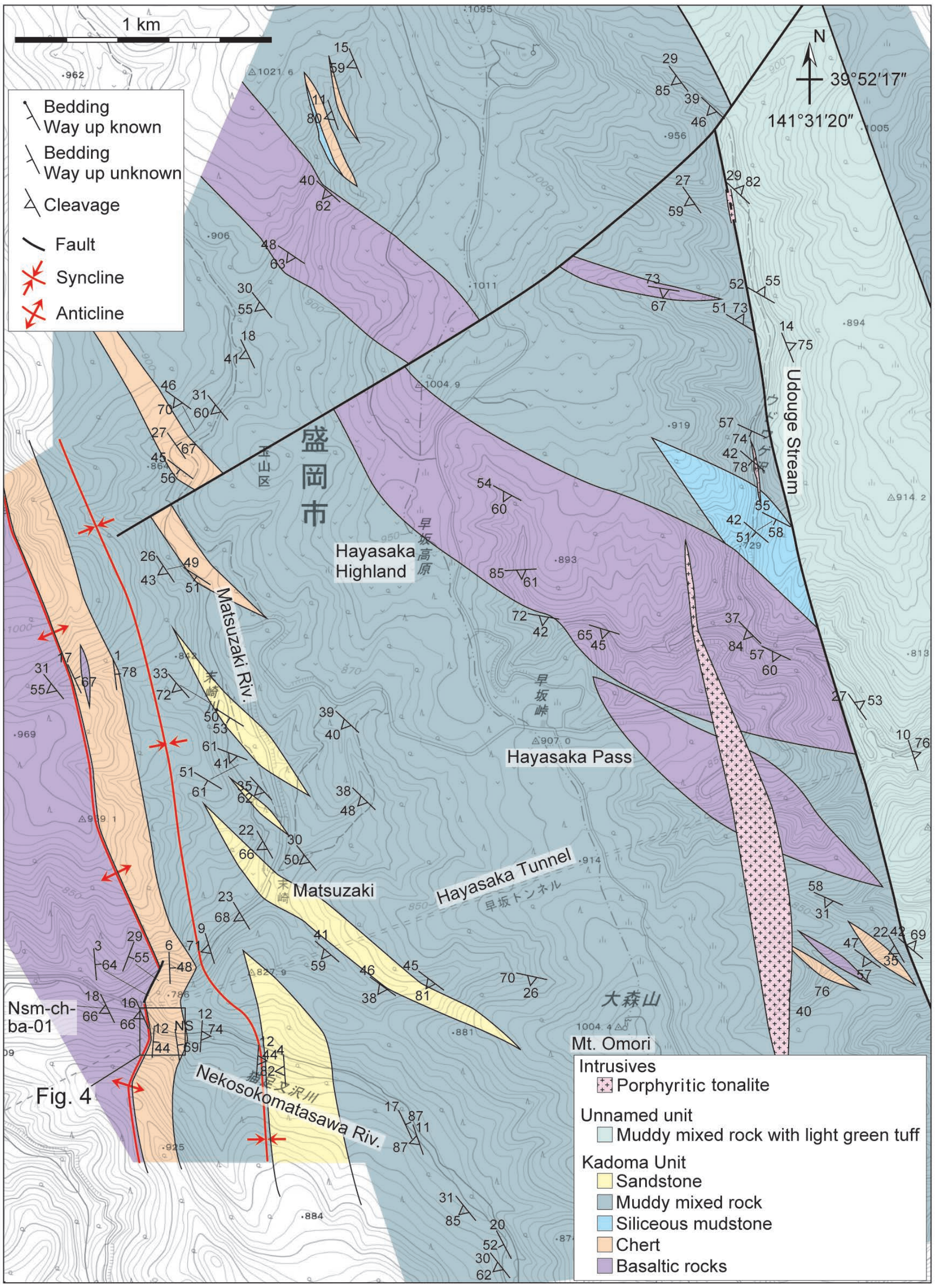

Fig. 2 - Geological map of the Hayasaka Highland. Sampling locality of sample Nsm-ch-ba-01 is shown. For other localities, see Fig. 3. Base map produced from XYZ tiles provided by the Geospatial Authority of Japan. Riv., River; Mt., Mount. The reader is referred to the PDF online for a colour version.

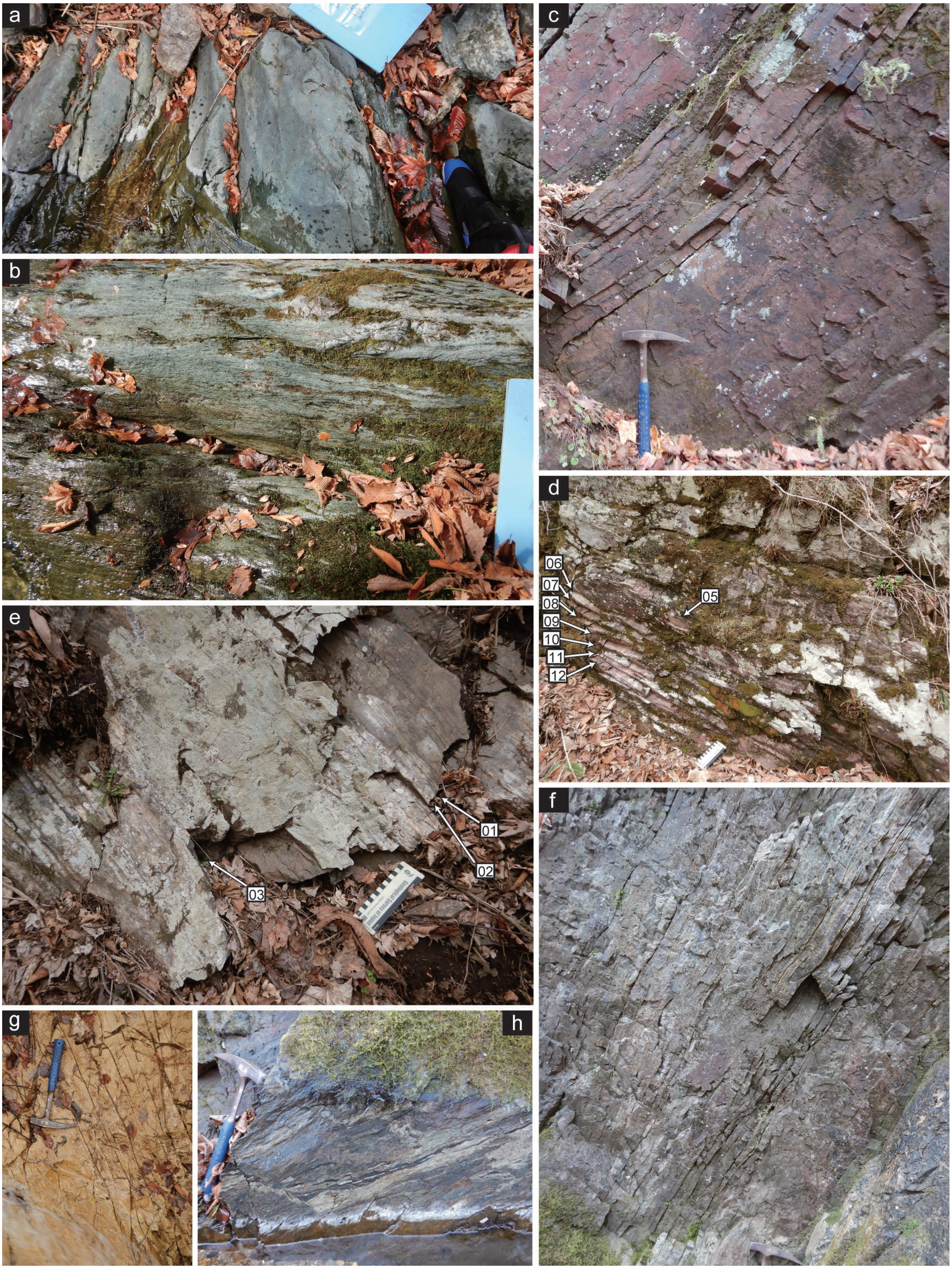

Fig. 3 - Field photographs of rocks around the Hayasaka Highland. a) Bedded basaltic lava. Matsuzaki River. b) Basaltic tuff. Matsuzaki River. c) Red bedded chert. Nekosokomatazawa River. d) Red bedded chert and e) grey bedded chert of the sampled section (see Figs. 4 and 5). Numbers indicate the last two digits of the sample ID that begins with "Nsm-ch-". f) Grey bedded chert. Nekosokomatazawa River. g) Weathered sandstone. Matsuzaki River. h) Muddy matrix of mixed rock facies containing abundant silty and tuffaceous deformed layers and fragments. Matsuzaki River. For scale, the blue board is 30 cm × 20 cm, the hammer is 30 cm long and the ruler is 10 cm.

The basalt and lower red chert units are exposed along the stream (Fig. 4). The basalt unit is composed of weakly foliated basaltic lava at least 5 m in apparent thickness (Fig. 5). The lower red chert unit is well-bedded and is apparently 18 m thick (Fig. 5). The stratigraphic contact between basaltic rocks and red bedded chert is not observed due to poor exposure and the presence of a minor fault. However, the occurrence of intermediate lithology (tuffaceous chert and siliceous basaltic tuff) in the structurally uppermost part of the basalt unit (Figs. 4, 5) implies that the observed lithofacies is part of a basalt-chert sequence with a gradual transition, and that the unobserved interval could be minor. We also note that the minor fault dividing the exposure of the basalt and lower red chert units is negligeable in the general geological structure of the study area (Fig. 2). The distribution of red and grey chert on both sides of the Neokosomatasawa River also indicates that the displacement of this fault is minor, probably less than 10 m (Fig. 4). The upper red chert and grey chert units are exposed along the logging road (Fig. 4). Both units are composed of well-bedded chert, and the apparent thickness is 14 m for the red chert unit and around 23 m for the grey chert unit (Fig. 5). The apparent thickness of the strata in the studied section may be different from the true stratigraphic thickness because faults and folds may be present in covered areas.

The basalt unit in the studied section is composed of basaltic lava, while basaltic tuffs were observed to the northwest along the Matsuzaki River. Basaltic lava in and around the study section is mostly intergranular (Fig. 6a-c, f-i) or intersertal (Fig. 6d), while amygdaloidal basalt occurs limitedly on the east side of the Hayasaka Highland. Plagioclase, largely saussuritized, is present in all samples. Some samples contain titanian augite and brown amphibole. Secondary minerals such as epidote, chlorite, actinolite, and sphene are present. Foliated varieties have seams partly filled with chlorite (Fig. 6d) and preserve less titanian augite or plagioclase. Basaltic tuff is composed of chlorite, saussuritized plagioclase, carbonate, quartz and abundant fine-grained opaque minerals and shows conspicuous asymmetric shear structures with no original sedimentary structures (Fig. 6e). Both red and grey cherts are composed of radiolarian tests in quartz matrix that are recrystallized (Fig. 6j-n). Conodont fossils are found in some thin sections of chert (Fig. 6j-n). Stubby micrometre-sized illite and biotite, formed from clay minerals, are present, indicating some degree of metamorphic effects from plutons.

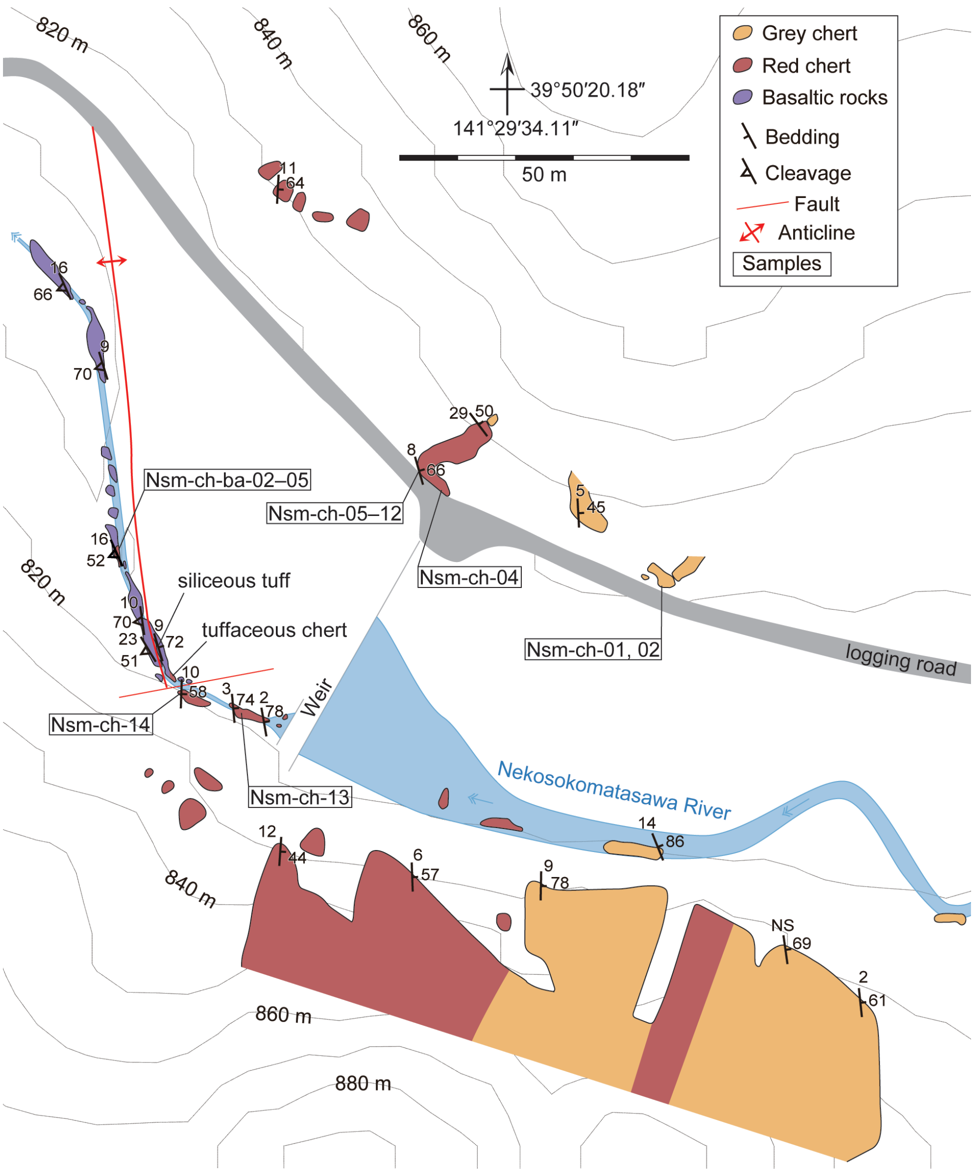

Fig. 4 - Plan-view field map around the studied section along the Nekosokomatasawa River. The lower and upper red chert units are not differentiated here. Sample Nsm-ch-ba-01 was obtained from outside this area. The reader is referred to the PDF online for a colour version.

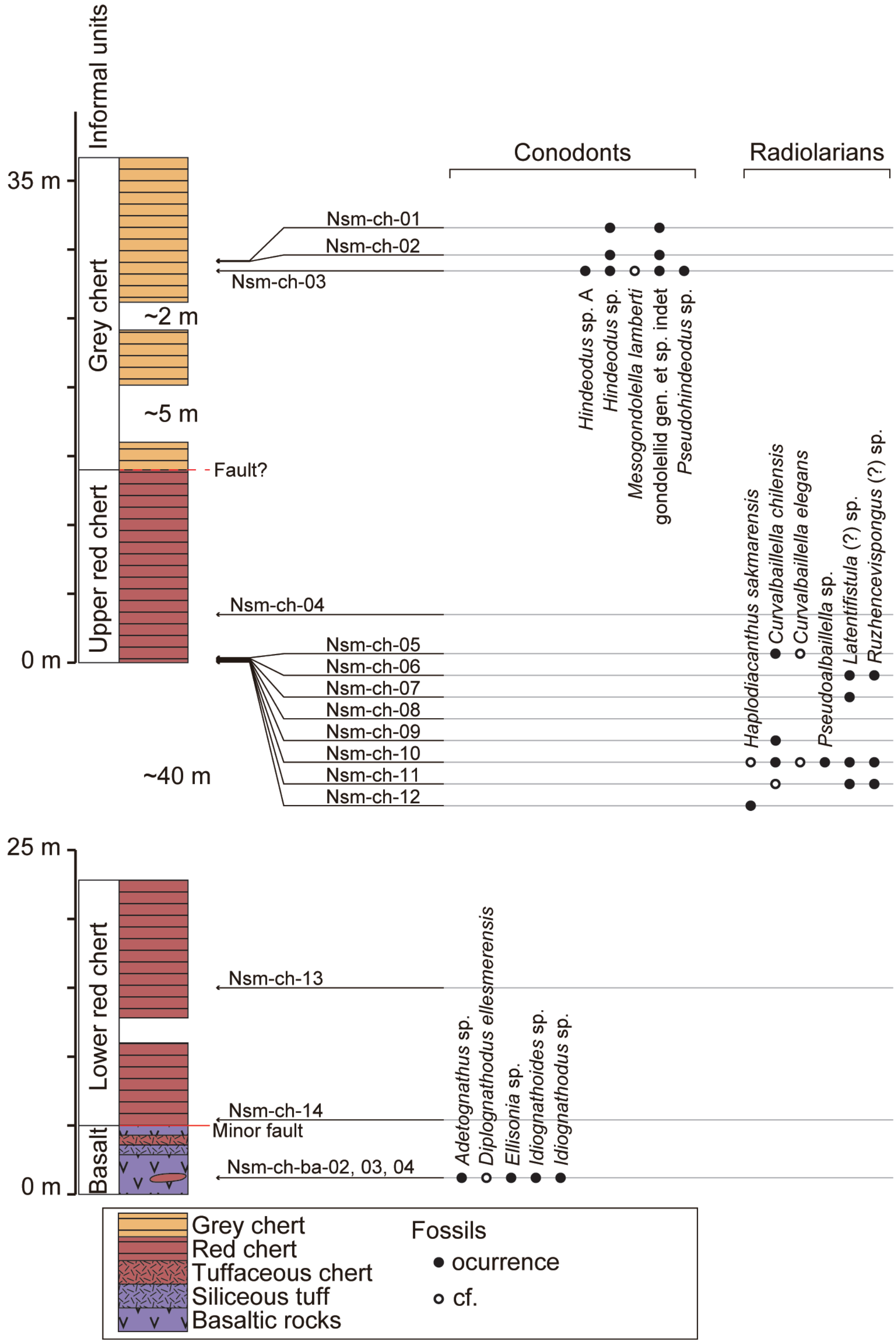

Fig. 5 - Lithologic column and fossil occurrences of the studied section. The column is based on apparent thickness at the outcrop which may be different from true stratigraphic thickness due to minor faults and folds. Gaps between columns are covered areas and may conceal faults and folds. Sample Nsm-ch-ba-05 is a basalt sample not treated for microfossils, and is not shown here. Gondolellids from sample Nsm-ch-03 include specimens that may be *Jinogondolella nankingensis tenuis* Wardlaw. The reader is referred to the PDF online for a colour version.

SAMPLES AND METHODS

We investigated 18 samples for microfossils. One sample (Nsm-ch-ba-01) was collected from the junction of the Matsuzaki and Nekosokomatasawa rivers to the west of the main study section (Fig. 2). This sample and the three samples (Nsm-ch-ba-02 to 04) from the basalt unit of the main study section are red nodular cherts embedded within green basaltic rocks (Figs. 2, 4). The boundary of chert and basaltic matrix is oblique to the foliation in the basaltic rocks (Fig. 7a, b). One of these samples (Nsm-ch-ba-02) had low transparency and may be classified as jasper. Two samples (Nsm-ch-13 and 14) were obtained from the lower red chert unit, nine samples (Nsm-ch-04 to 12) were obtained from the upper red chert unit and three samples (Nsm-ch-01 to 03) were obtained from the grey chert unit (Figs. 4, 5).

Samples were crushed into cm-size pieces and treated with 5 % hydrofluoric (HF) acid for 24 hours, repeated over four cycles. The residue was inspected under a stereoscopic microscope and fossils were hand-picked using a fine brush. After this initial treatment, samples from red nodular chert in basaltic rocks and grey bedded chert yielded only scant, pale-colored and fractured conodont fossils and no radiolarians. These samples were subsequently treated by 10% HF acid for 6 to 18 hours over more than twelve cycles. This additional treatment resulted in more numerous and intact conodonts. Picked fossils were mounted on metal stubs, coated with carbon and photographed by a scanning electron microscope (SEM; Hitachi SU3500) at the Geological Survey of Japan, AIST.

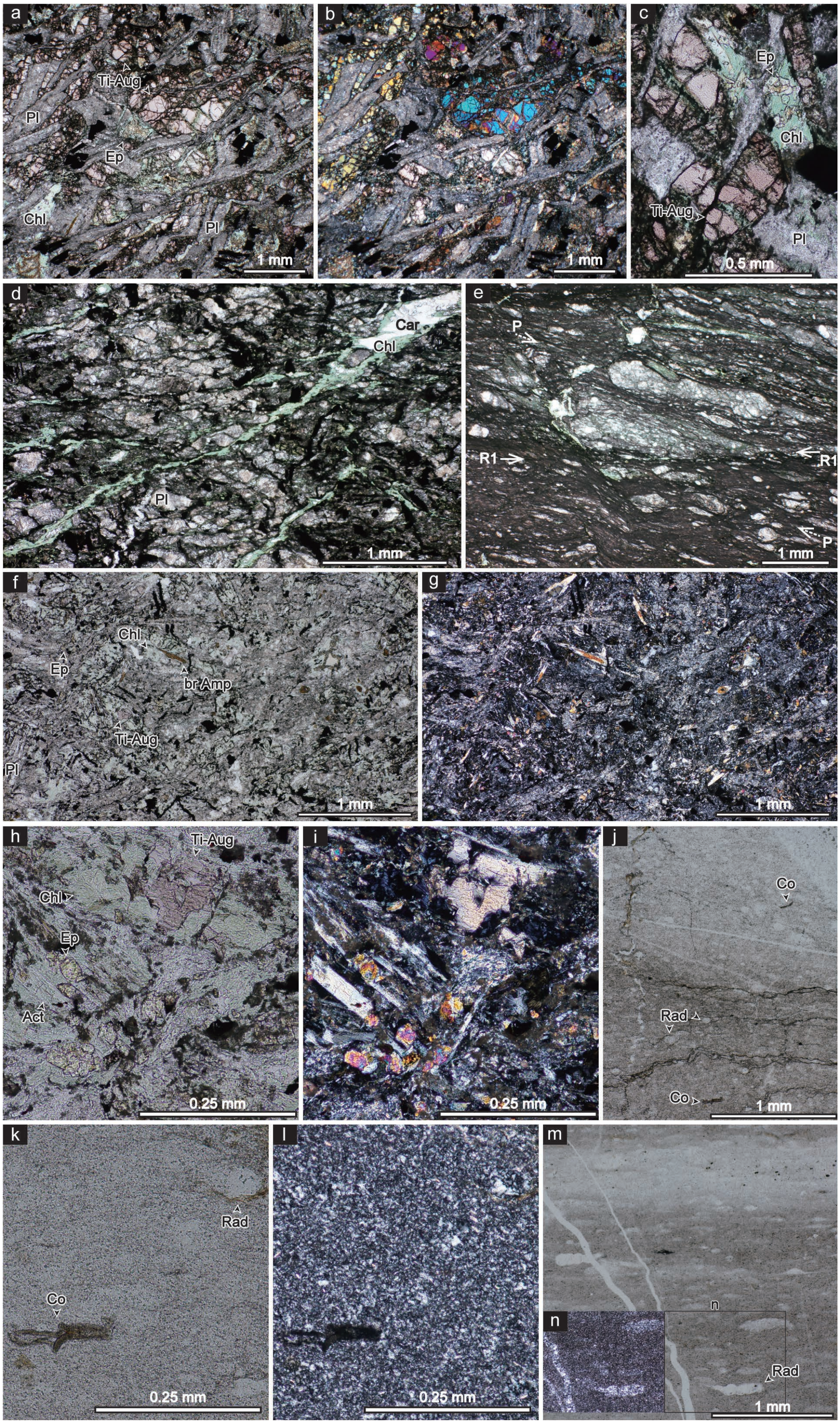

Fig. 6 - Thin section micrographs of basaltic and siliceous rocks around the studied section. a, b, c) Green massive basaltic lava. Same field of view for a) and b). Matsuzaki River. d) Green basaltic lava with moderate foliation. Matsuzaki River. e) Green basaltic tuff with strong foliation. Asymmetric shear structures characterized by P and R1 planes are observed. Matsuzaki River. f, g, h, i) Green basaltic lava with moderate foliation. Sample Nsm-ch-ba-05. Same field of view for f) and g), and h) and i), respectively. j, k, l) Grey bedded chert (Sample Nsm-ch-03). Same field of view for k) and l). m, n) red bedded chert. Sample Nsm-ch-09. a, b, c, e, f, h, j, k, m: plane-polarized light. d, g, i, l, m: cross polarized light. Act: actinolite; br-Amp: brown amphibole; Car: carbonate; Chl: chlorite; Ep: epidote; Pl: plagioclase; Ti-Aug: titanian augite; Co: conodont; Rad: radiolarian test.

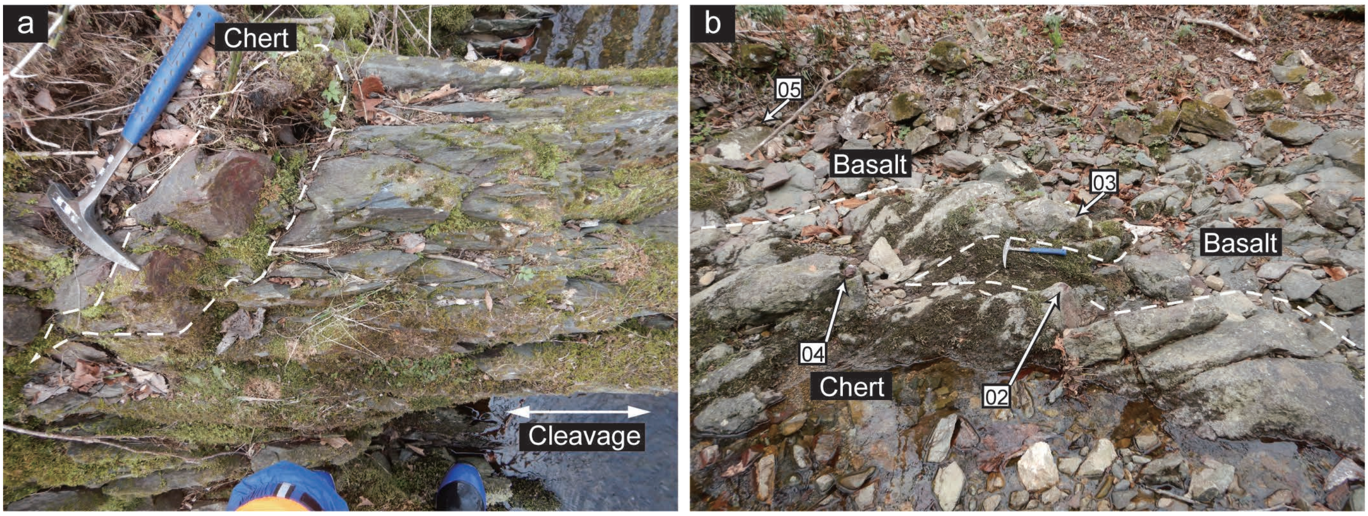

Fig. 7 - Field photographs of red chert enclosed in basaltic rocks. a) Red chert lens within foliated basaltic rocks. Matsuzaki River. The lithological boundary intersects at an angle to the cleavage in the basaltic rocks. b) Red chert block with an irregular boundary with basaltic rocks. Numbers indicate the last two digits of the sample ID that begins with "Nsm-ch-ba-". The hammer for scale is 30 cm long.

MICROFOSSIL OCCURRENCE

Conodonts

Conodonts were obtained from nodular red chert within basaltic rocks of the basalt unit, the lowermost part of the red chert unit and the middle part of the grey chert unit (Fig. 5; Table 1). Conodont fossils are pale brown colored and recrystallized possibly due to reaction with HF acid. Most of the identifiable fossils were obtained from two samples: sample Nsm-ch-ba-02 from nodular red chert in basalt and sample Nsm-ch-03 from grey bedded chert.

Of the nodular red chert samples, only one (Nsm-ch-ba-02) yielded conodonts (Table 1). This sample contained *Idiognathodus* sp., *Idiognathoides* sp., *Diplognathodus* sp. cf. *D. ellesmerensis* Bender, *Ellisonia* sp., *Adetognathus* sp. and other unidentifiable elements (Fig. 8). Unidentified elements include a broken platform similar to that of *Idiognathoides sulcatus* Higgins and Bouckaert (Fig. 8y) and a carminiscaphate element with a blade apparently higher than the platform that may be a species of *Diplognathodus* (Fig. 8bb). Identification at the species level was difficult due to the poor preservation of the fossils. Aside from conodonts, the nodular red chert samples including sample Nsm-ch-ba-02 yielded sponge spicules, suggesting that the silica component of the chert nodules are at least partly derived from biogenic silica (Fig. 9s-x). Of the grey chert samples, sample Nsm-ch-03 yielded *Mesogondolella* sp. cf. *M. lamberti* Mei and Henderson, *Hindeodus* sp. A, *Hindeodus* sp. *Pseudohindeodus* sp. (Fig. 5; 8b, c, i-r; Table 1) and fragments of gondolellid P1 elements (Fig. 8a, d-h). Although questionable, two of the gondolellid elements (Fig. 8d, f) may belong to *Jinogondolella nankingensis tenuis* Wardlaw, judging from the narrow platform and long proclined cusp (Wardlaw, 2015). Elements of *Hindeodus* and gondolellids were also obtained from the other two grey chert samples.

The age of the basaltic rocks in the studied section is constrained by the occurrence of *Idiognathoides* sp. and *Diplognathodus* sp. cf. *D. ellesmerensis* Bender from sample Nsm-ch-ba-02. *Idiognathoides* is a cosmopolitan taxon that appeared in the early Bashkirian and disappeared in the early Moscovian (Lane and Straka, 1974; Nemyrovskaya, 1999; 2017; Barrick et al., 2013; Hu et al., 2020a). Our specimen is a juvenile specimen, probably of *Idiognathoides sinuatus* (Harris and Hollingsworth), the range of which parallels the entire range of the genus. *Diplognathodus ellesmerensis* is also a widespread taxon known to occur from the uppermost Bashkirian to middle Moscovian (Bender, 1980; Nemyrovskaya, 1999; 2017; Hu et al., 2020b). Notably, Hu et al. (2020b) proposed the first appearance of this species as a marker for the base of the Moscovian. Regarding our conodonts, *Diplognathodus* sp. cf. *D. ellesmerensis* is represented only by one rather poorly preserved specimen and should not be overemphasized. Therefore, we conclude that the age of the basalt unit is likely to be early Moscovian and is certainly within the Bashkirian to early Moscovian. The other conodont fossils are in accordance with this age assignment. *Idiognathodus* occurs throughout the Bashkirian to Gzhelian (e.g., Barrick et al., 2013; 2023), *Adetognathus* occurs from the Bashkirian to Asselian (e.g., Dunn, 1970; Hu et al., 2020a; Beauchamp et al., 2022a; 2022b) and *Ellisonia* is known from Bashkirian to Anisian (lower Middle Triassic) (von Bitter and Merril, 1983; Koike, 2016; Muto et al., 2023c).

The age of the grey chert unit is constrained by the occurrence of *Mesogondolella* sp. cf. *M. lamberti* and *Pseudohindeodus* sp. *Mesogondolella lamberti* is a well-known taxon that indicates a short age interval in the latest Kungurian to earliest Roadian in low latitudes (Mei and Henderson, 2002; Lambert et al., 2007; Wardlaw, 2000; 2015; Metcalfe, 2023). Currently known species of *Pseudohindeodus* are found from the Artinskian through to Wordian (Igo, 1981; Orchard and Forster, 1988; Wardlaw, 2000; Wardlaw and Nestell, 2015; Henderson, 2018; Sun et al., 2017). We also found gondolellid P1 elements that may belong to *Jinogondolella nankingensis tenuis* Wardlaw. This subspecies occurs from the Roadian to lowermost Wordian (Wardlaw, 2015). Although our specimens are not confidently identified because the ventral half is missing, the occurrence of this subspecies would not contradict with the presence of *Mesogondolella* sp. cf. *M. lamberti* and *Pseudohindeodus*. Species of *Hindeodus* from this sample do not provide further age constraints. This genus has a very long range from the early Carboniferous to the Early Triassic (e.g., Sweet et al., 1977). Some species are known as age indicators, but our specimens cannot be assigned to such species. In sum, the age of the grey bedded chert includes the latest Kungurian or earliest Roadian.

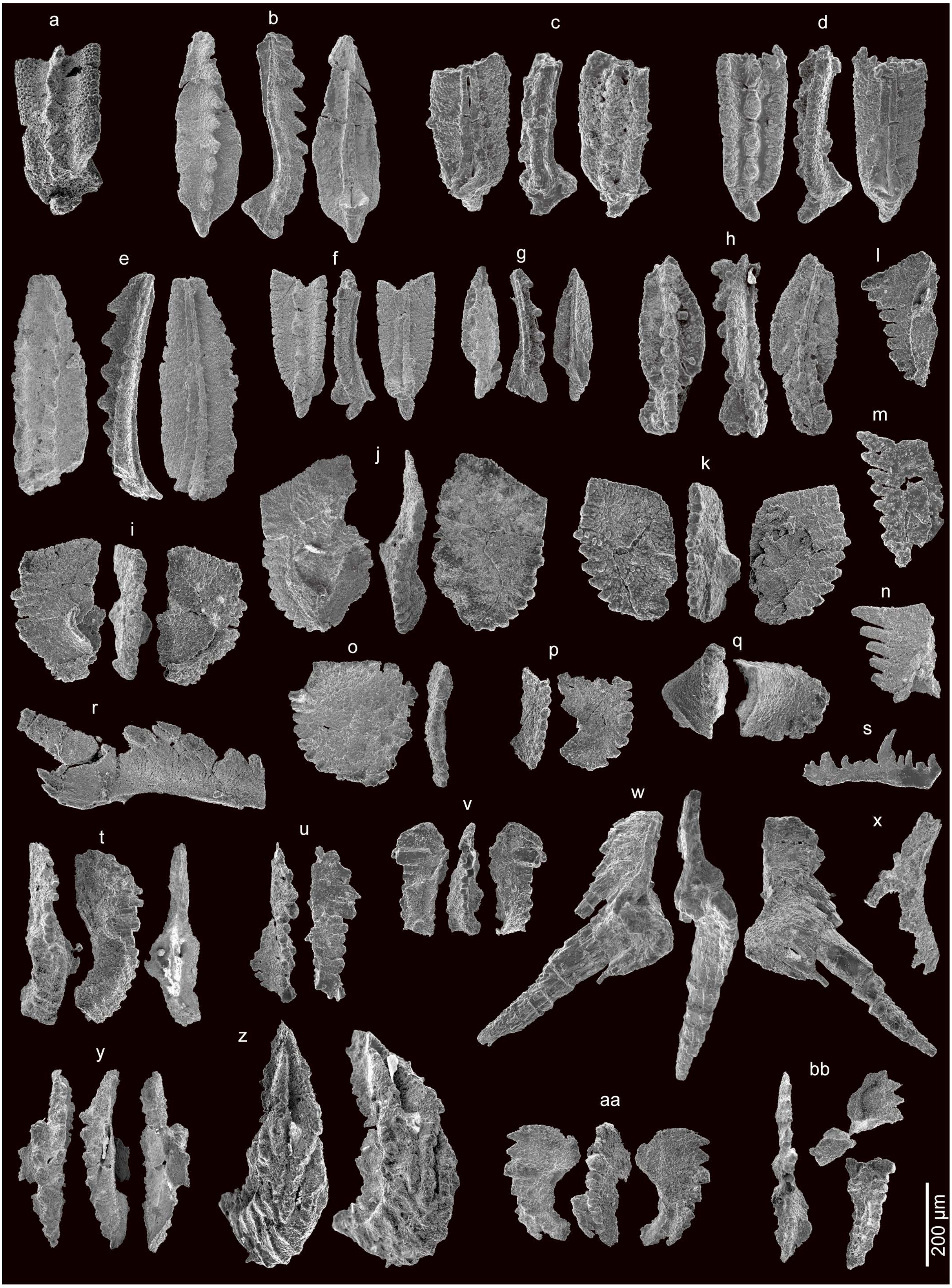

Fig. 8 - Conodonts obtained from the studied section. Scale bar is 200 μm. a, e, g, h) gondolellid gen. et sp. indet. P1 element. a: Nsm-ch-02; e, g, h: Nsm-ch-03. b, c) *Mesogondolella* sp. cf. *M. lamberti* Mei and Henderson. Nsm-ch-03. d, f) *Jinogondolella nankingensis tenuis* Wardlaw? Nsm-ch-03. i, k) *Hindeodus* sp. A. Nsm-ch-03. j, l-p) *Hindeodus* sp. Nsm-ch-03. q) *Pseudohindeodus* sp. Nsm-ch-03. r) angulate (gondolellid P2?) element. Nsm-ch-03. s) bipennate element. Nsm-ch-14. t) *Idiognathoides* sp. Nsm-ch-ba-02. u) *Diplognathodus* sp. cf. *D. ellesmerensis* Bender. Nsm-ch-ba-02. v, aa) *Adetognathus* sp. Nsm-ch-ba-02. w) *Ellisonia* sp. Nsm-ch-ba-02. x) angulate element (*Ellisonia* sp.?). Nsm-ch-ba-02. y, bb) carminiscaphate element. Nsm-ch-ba-02. z) *Idiognathodus* sp. Nsm-ch-ba-02.

Table 1 - Occurrence list of conodonts and radiolarians in this study.

	Conodonts												Radiolarians										
Sample no.	*Adetognathus* sp.	*Diplognathodus* sp. cf. *D. ellesmeransis* Bender	*Ellisonia* sp.	*Idiognathoides* sp.	*Idiognathodus* sp.	*Hindeodus* sp. A	*Hindeodus* sp.	*Mesogondolella* sp. cf. *M. lamberti* Mei and Henderson	*Jinogondolella nankingensis tenuis* Wardlaw	*Pseudohindeodus* sp.	gondolellid gen. et sp. indet.	unidentified elements	Follicucullidae (?) gen. et sp. indet.	Follicucullidae gen. et sp. indet.	*Haplodiacanthus sakmarensis* (Kozur)	*Haplodiacanthus* sp. cf. *H. sakmarensis* (Kozur)	*Curvalbaillella chilensis* (Ling and Forsythe)	*Curvalbaillella* sp. cf. *C. chilensis* (Ling and Forsythe)	*Curvalbaillella* sp. cf. *C. elegans* (Ishiga and Imoto)	*Pseudoalbaillella* sp.	*Latentifistula* (?) sp.	*Ruzhencevispongus* (?) sp.	Spherical radiolarian
Nsm-ch-01							+				+	+											
Nsm-ch-02							+				+	+											
Nsm-ch-03						+	+	+	?	+	+	+											
Nsm-ch-04													+										
Nsm-ch-05													+	+			+	+	+				+
Nsm-ch-06														+							+	+	
Nsm-ch-07													+								+		
Nsm-ch-08													+	+									+
Nsm-ch-09													+	+			+						
Nsm-ch-10													+	+		+	+	+	+	+	+	+	+
Nsm-ch-11													+	+				+			+	+	
Nsm-ch-12													+	+	+								+
Nsm-ch-13																							
Nsm-ch-14												+											
Nsm-ch-ba-01																							
Nsm-ch-ba-02	+	+	+	+	+							+											
Nsm-ch-ba-03																							
Nsm-ch-ba-04																							

Radiolarians

Radiolarians were obtained from the lowermost part of the upper red chert unit (samples Nsm-ch-04 through Nsm-ch-12; Fig. 5; Table 1). Although fossil preservations are generally poor, some radiolarians such as *Haplodiacanthus sakmarensis* (Kozur), *Haplodiacanthus* sp. cf. *H. sakmarensis* (Kozur), *Curvalbaillella chilensis* (Ling and Forsythe), *Curvalbaillella* sp. cf. *C. chilensis* (Ling and Forsythe) and *Curvalbaillella* sp. cf. *C. elegans* (Ishiga and Imoto) were identified. *Haplodiacanthus sakmarensis* is characteristic species of UAZ 4 (*H. sakmarensis* Interval Zone, originally *Pseudoalbaillella sakmarensis* Interval Zone) of Xiao et al. (2018). The FO of *H. sakmarensis* defines the base of UAZ 4. According to the statistic likelihood ranges of Xiao et al. (2018), *H. sakmarensis* occurs in UAZ 4 to UAZ 7, *C. chilensis* in UAZ 1 to UAZ 4 and *C. elegans* in UAZ 2 to UAZ 3. The co-occurrence of *H. sakmarensis*, *C. chilensis* and specimens compared to these species indicates that the samples are within UAZ 4. The samples are likely within the lower part of this zone, which is correlated to the middle Sakmarian, considering the occurrence of *Curvalbaillella* sp. cf. *C. elegans*.

The ranges of *C. chilensis* and *C. elegans* are known to be lower than that of *H. sakmarensis*, with overlaps in the middle Sakmarian. Hence, there is a possibility that the sampled interval between Nsm-ch-05 and Nsm-ch-12 is overturned due to unconfirmed folds and/or faults. However, because the interval has only a thickness of ~35 cm, we tentatively propose that it represents the overlap of the ranges of the above mentioned taxa, and assume no overturning of strata.

AGE OF THE OCEANIC PLATE

The studied section is dated as Bashkirian or early Moscovian to latest Kungurian or earliest Roadian based on the occurrence of conodonts and radiolarians (Fig. 10). The age of

Fig. 9 - Radiolarians (a-r) and sponge spicules (s-x) obtained from the studied section. a) *Haplodiacanthus sakmarensis* (Kozur). Nsm-ch-12. b) *Haplodiacanthus* sp. cf. *H. sakmarensis* (Kozur). Nsm-ch-10. c) *Pseudoalbaillella* sp. Nsm-ch-10. D-g) *Curvalbaillella chilensis* (Ling and Forsythe). d: Nsm-ch-09; e-g: Nsm-ch-10. h, i) *Curvalbaillella* sp. cf. *C. chilensis* (Ling and Forsythe). h: Nsm-ch-10; i: Nsm-ch-05. j, k) *Curvalbaillella* sp. cf. *C. elegans* (Ishiga and Imoto). Nsm-ch-05. l-o) *Latentifistula* (?) sp. l: Nsm-ch-10; m, o: Nsm-ch-11; n: Nsm-ch-12. P-r) *Ruzhencevispongus* (?) sp. p: Nsm-ch-12; q: Nsm-ch-10; r: Nsm-ch-06. s, t) monaxon. s: Nsm-ch-ba-01; t: Nsm-ch-ba-02. u) orthotriaene? Nsm-ch-ba-01. v) acanthostyle. Nsm-ch-ba-02. w) style? Nsm-ch-ba-02. x) triaxon (hexactine). Nsm-ch-ba-02.

the basalt unit is early Moscovian or, less likely, Bashkirian and the age of the lower part of the upper red chert unit is Sakmarian, probably its middle part. The lower red chert unit has not yielded any age diagnostic fossils.

As far as the distribution of lithofacies, geological structure and microfossil data show, there is no reason to assume that the stratigraphic position of the lower red chert unit is different from its structural position, which is between the basalt and upper red chert units. Accordingly, we speculate that the age of the lower red chert unit is within the Moscovian to Sakmarian interval. The age of the sampled horizon of the grey chert unit is latest Kungurian or earliest Roadian. Therefore, the upper part of the upper red chert unit and the grey chert unit encompass the Artinskian to Kungurian. Grey bedded chert continues to occur above our studied section (Fig. 4). Since Matsuoka (1988) reported radiolarians of late Sinemurian or early Pliensbachian (Early Jurassic) from black chert of the Kadoma Unit, the entire age range of bedded chert in this unit is Pennsylvanian to Early Jurassic.

While there have been countless works on the age of bedded chert within the Jurassic accretionary complex of Japan, this is the first report to indicate the age of the underlying basaltic rocks based on direct evidence. Previously, the age of the basal basaltic rocks has been suggested based on the occurrence of Pennsylvanian radiolarians and conodonts from bedded chert (detailed below), some of which are associated with basaltic rocks, but the basal basaltic rocks themselves had not been dated directly. We thus provide the first solid evidence that the oceanic plate stratigraphy of the Jurassic accretionary complex of Japan has, at least partly, Pennsylvanian basaltic rocks as its foundation.

Here we summarize previous works that provide information on the age of sedimentary rocks close to the basaltic basement in the oceanic plate stratigraphy of the Japanese Jurassic accretionary complex (Fig. 10; see also Fig. 1b for location). These studies do not give dates for the basaltic rocks themselves, but they do provide evidence for the minimum age. Bedded chert associated with basaltic rocks from the Otori Unit, a younger accretionary unit in the North Kitakami Belt in the Akka area, yielded Moscovian conodonts, which is the same case as our study section (Muto et al., 2023b). Older conodonts of Bashkirian age were reported from two sections in the Tanba Belt in Southwest Japan: red bedded chert and red siliceous or tuffaceous mudstone associated with basalt in Sasayama (Ishiga, 1982) and a succession of red mudstone, red chert and dolostone in Kameoka (Imoto et al., 1997). Meanwhile, even older fossil assemblages indicating the Visean or Serpukhovian have been reported from limestone and chert in the Northern Chichibu Belt in Shikoku (Ishida, 1985) and the Southern Chichibu Belt in Kanto (Igo and Kobayashi, 1974) and Shikoku (Ishida, 1979), although localities of the Northern Chichibu Belt may belong to Permian accretionary complexes. Furthermore, Ito and Matsuoka (2018) studied the Ryokami-yama Chert Formation, a component of the Southern or Northern Chichibu Belt in the Kanto Mountains, where they found Sakmarian radiolarians from red bedded chert overlying basaltic rocks. They also demonstrated that the oldest age of bedded chert is Sakmarian in many other localities in the Jurassic accretionary complex of Japan and suggested that Sakmarian basaltic rocks constituted a significant part of the oceanic plate. Based on the above studies, the age of basaltic rocks forming the oceanic plate in the Jurassic accretionary complex of Japan is not uniform, and has an age range of Serpukhovian or older to Sakmarian, a span of ~ 40 million years or longer.

The age data of non-basaltic rocks provided by previous studies need to be considered with caution. For example, Kusunoki et al. (2004) reported the occurrence of hyaloclastite and dolostone including basaltic fragments near the bottom of a chert and dolostone dominated sequence in Shizugawa, southeast Kyoto, which yielded Gzhelian to Asselian fossils. Their studied section belongs to a tectonostratigraphic unit called the Shuzan Unit (sensu Nakae, 2000), and its western extension in Kameoka, southwest Kyoto was studied by Imoto et al. (1997). While Permian to Jurassic components of the Shuzan Unit in both study areas are similar, Imoto et al. (1997) reported older, Bashkirian conodonts (Fig. 10). Hence, the basaltic rocks in Shizugawa probably represent hyaloclastic input from oceanic volcanoes onto already accumulated pelagic sediments, rather than from a mid-oceanic ridge. If the occurrence of carbonates is indicative of inputs from oceanic volcanoes, then age data from Imoto et al. (1997), Muto et al. (2023b) and Ito and Mastuoka (2018) may also not represent the age of the oceanic plate. Geochemical analysis of the basaltic rocks is likely to resolve this problem.

We also note that the taxonomy of conodonts in some of the older works need to be reevaluated, partly because taxonomic concepts have been revised since then. While Carboniferous conodont studies date back to the pioneer works in the USA in the 1930s (e.g., Gunnel, 1931), intense studies after the 1980s were required to construct a global framework of correlation (e.g., Ritter, 1995; Nemyrovskaya, 1999; Wang and Qi, 2003: Chernykh, 2005). Early Permian conodont studies have a shorter history, and monographic

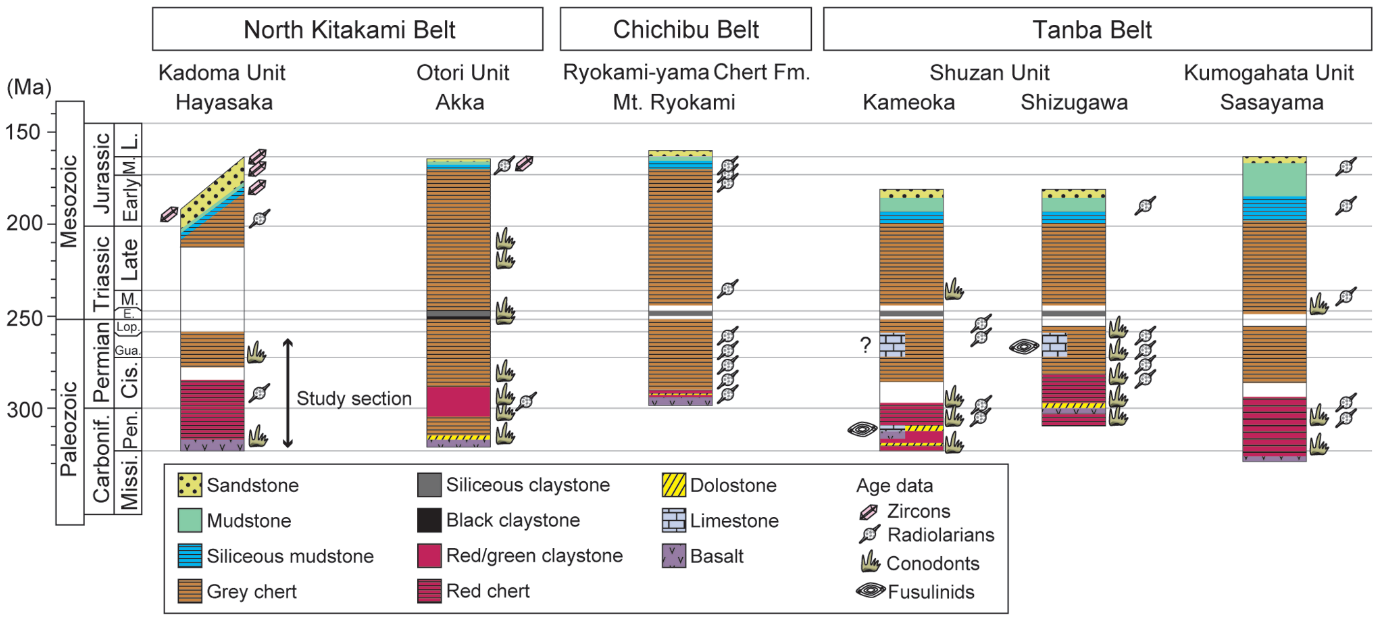

Fig. 10 - Reconstructed oceanic plate stratigraphy of the Kadoma Unit compared with other tectonostratigraphic units of the Jurassic accretionary complex of Japan with good age constraints for the older part of the oceanic rocks. Age data after this study, Uchino (2019; 2021a) and Osaka et al. (2023) for the Kadoma Unit, Muto et al. (2023a; 2023b) for the Otori Unit, Ito and Matsuoka (2018) for the Ryokami-yama chert Formation (Ryokami-yama is the Japanese for Mt. Ryokami in Fig. 1B), Imoto et al. (1997) and Miyachi et al. (2005) for the Shuzan Unit in Kameoka, Kusunoki et al. (2004) and Wakita et al. (2013) for the Shuzan Unit in Shizugawa and Ishiga (1982) and Kurimoto et al. (1993) for the Kumogahata Unit in Sasayama. The Ryokami-yama chert Formation has been ascribed to units in the Southern Chichibu or Northern Chichibu Belt, but the debate is not settled (Yoshida and Matsuoka, 2003). We adopted the unit division by Nakae (2000) for the Tanba Belt, while the local names for the Shuzan and Kumogahata units in the areas where the older part of the oceanic plate stratigraphy was studied are the “Tano” and “Sanaka” units respectively (Kurimoto et al., 1993; Miyachi et al., 2005). The occurrence of Permian carbonates in southwest Kyoto is illustrated in lithological columns in Miyachi et al. (2005), but supporting fossil images or localities are not shown. Timescale from International Chronostratigraphic Chart v2023/06 (Cohen et al., 2013; updated). Carbonif.: Carboniferous; Missi.: Mississippian; Pen.: Pennsylvanian; Cis.: Cisuralian; Gua.: Guadalupian; Lop.: Lopingian; E.: Early; M.: Middle; L.: Late. The reader is referred to the PDF online for a colour version.

works in the 2000s such as Chernykh (2006) and Boardman et al. (2009) were vital for international correlation. Regarding the Japanese studies referenced above, *Idiognathoides sinuatus* (Harris and Hollingsworth) (author erroneously shown as Gunnell therein) in Figs. 4 and 6 of Plate 2 in Ishiga (1982) is *Idiognathoides planus* Furduj, judging from the dorsally convex transverse ridges and very short medial trough. Ishiga (1982) also showed two elements identified as *Gnathodus roundyi* Gunnell, but the carina deflecting to one side of the platform in the dorsal portion indicates that these forms would now be placed in *Declinognathodus* (e.g., Nemyrovska, 1999). *Streptognathodus elongatus* Ellison was identified in the paper, which was a name used for narrow forms from a wide stratigraphic range. The forms illustrated therein probably do not include *S. elongatus* of the present taxonomic understanding and includes species such as *Streptognathodus constrictus* Reshetkova and Chernykh (Pl. 2 Fig. 13 of Ishiga, 1982; see e.g., Boardman et al., 2009). *Idiognathodus delicatus* Gunnell was also recognized in Ishiga (1982), but this is another name to which multiple taxa from a variety of ages has been assigned. The two specimens therein have a medial trough on the platform and therefore is not *Idiognathodus*, and one of them with a short carina and low parapets (Pl. 2 Fig. 9 of Ishiga, 1982) is a species of *Swadelina* (Lambert et al., 2003). Although the taxonomic revision above does not greatly alter the age assignment in this case, such reassessment of older literature is required to revive their valuable information.

In summary, the age of formation of the oceanic plate incorporated in the Jurassic accretionary complex of Japan indicates partly Early Pennsylvanian and partly Late Mississippian or older ages. At the moment, it is premature to establish systematic relationships between the age of the basaltic basement of the oceanic plate and other characteristics of the accretionary complex, such as geotectonic divisions or accretionary age (Fig. 10). Basaltic rocks from other localities that are not associated with carbonates need to be investigated for fossil-yielding chert nodules.

CONCLUSIONS

We investigated the lithostratigraphy and biostratigraphy of a basalt-chert sequence in the Jurassic accretionary complex of the North Kitakami-Oshima Belt. The study section represents the lower portion of the oceanic plate stratigraphy of the accretionary complex in the area. A red chert nodule within basaltic rocks yielded conodonts that may be Bashkirian or, more likely, early Moscovian in age (late Carboniferous). Red bedded chert above the basaltic rocks yielded Sakmarian (early Permian) radiolarians and grey bedded chert further above yielded conodonts that indicate the latest Kungurian to earliest Roadian (end early Permian to earliest middle Permian). Carboniferous basalt overlain by upper Carboniferous to Permian bedded chert has been considered to be the typical lithology of the lower part of the oceanic plate stratigraphy in the Jurassic accretionary complex, but this study provides the first direct age evidence for the basaltic rocks at the base. The entire age range of the oceanic plate incorporated in the Jurassic accretionary complex of Japan spans tens of millions of years, with the oldest parts at least as old as the Serpukhovian and younger parts perhaps as young as the Sakmarian early Carboniferous.

TAXONOMIC NOTES

Conodonts (by Shun Muto)

Genus ***Adetognathus*** Lane, 1967
Type species ***Cavusgnathus lautus*** Gunnell, 1933

***Adetognathus* sp.** (Fig. 8v, aa)
Remarks: The specimens are carminiscaphate elements with a lateral junction of the blade and platform. The long free blade joining smoothly with one raised platform margin and wide medial trough on the platform are characteristic of this genus. There appears to be a large denticle slightly ventrally to the termination of the platform in both specimens, but it is not certain due to recrystallization.

Genus ***Diplognathodus*** Kozur, 1975
Type species ***Spathognathodus coloradoensis***
Murray and Chronic, 1965

Diplognathodus* sp. cf. *D. ellesmerensis Bender (Fig. 8u)
1980 *Diplognathodus ellesmerensis* - Bender, p. 9-10, Pl. 4, Figs. 5-7, 11, 15-17, 19-21, 23-25.
Remarks: Our specimen is a carminiscaphate element with a ventral blade and dorsal thin-walled platform. The platform bears a carina of sub-equal height composed of round-topped denticles. The blade is at least as long as the platform and distinctly higher than the carina. A low point (notch) exists between blade and carina where a small denticle is present. The height of the blade against the carina and the flat outline of the carina distinguishes this form from other *Diplognathodus*, but the preservation is somewhat poor. Typical *D. ellesmerensis* has two to four denticles in the notch, while the present specimen has only one, perhaps due to its small size. See Hu et al. (2020b) for synonymy.

Genus ***Ellisonia*** Müller, 1956
Type species ***Ellisonia triassica*** Müller, 1956

***Ellisonia* sp.** (Fig. 8w)
Remarks: The specimen is an angulate element with a reduced posterior process. The denticles are discrete. The cusp is more than three times higher and thicker than other denticles. The basal area is conspicuously upturned in one side.

Genus ***Hindeodus*** Rexroad and Furnish, 1964
Type species ***Trichonodella imperfecta*** Rexroad, 1957

***Hindeodus* sp. A** (Fig. 8i, k)
Remarks: These specimens have a high fused blade with thin round-topped denticles. The basal cavity has a characteristic pinched fold on the upper surface. The portion of the basal cavity dorsal of this fold is laterally restricted. The cusps of the present specimens are broken at the base, where it is twice as thick as the other denticles. *Hindeodus ellisoni* (Merrill, 1973) also has thin numerous denticles, but are dorso-ventrally longer and lack the fold on the upper surface of the basal cavity. Other unidentified elements of *Hindeodus* found in this study include forms with highly fused blades like that of *Hindeodus* sp. A (Fig. 8j, o, p) and forms with more discrete blades (Fig. 8l-n).

Genus ***Idiognathodus*** Gunnell, 1931
Type species ***Idiognathodus claviformis*** Gunnell, 1931

***Idiognathodus* sp.** (Fig. 8z)
Remarks: This specimen is deformed with its platform twisted and broken at the junction of the blade and platform. A long carina stands between parapets. At least one side bears a nodose lobe. Transverse ridges crossing the platform are uninterrupted.

Genus ***Idiognathoides*** Harris and Hollingsworth, 1933
Type species ***Idiognathoides sinuata***
Harris and Hollingsworth, 1933

***Idiognathoides* sp.** (Fig. 8t)
Remarks: The specimen is a carminiscaphate element with a lateral junction of the blade and platform. The platform is crossed by transverse ridges and lacks a medial trough. A short caudal parapet is present. The untroughed posterior platform and length of the caudal parapet makes this specimen most similar to *Idiognathoides sinuatus* (Harris and Hollingsworth). Adult specimens of *Idiognathodus attenuatus* (Harris and Hollingsworth) can be distinguished by the very short medial trough, and *Idiognathoides asiaticus* Nigmadganov and Nemirovskaya by the coarser transverse ridges. However, the present specimen is a juvenile and the preservation is somewhat poor, and therefore specific identification is avoided.

Genus ***Mesogondolella*** Kozur, 1989
Type species ***Gondolella bisselli*** Clark and Behnken, 1971

Mesogondolella* sp. cf. *M. lamberti Mei and Henderson, 2002 (Fig. 8b, c)
2002 *Mesogondolella idahoensis lamberti* - Mei and Henderson, p. 533-534, Pl. 1, Fig. 10, Pl. 2, Figs. 1-17.
Remarks: The specimen illustrated in Fig. 8b has a platform widest near the middle, tapering to the ventral end and narrowing slightly to the rounded dorsal end. The carina is moderately fused in the ventral portion and the distinguishable cusp reclines over the dorsal end. The basal area of the cusp creates a slight protrusion of the dorsal brim of the platform. The specimen illustrated in Fig. 8c is broken in the ventral portion, but the outline of the dorsal platform and denticulation match the features of this species. Both specimens are from juvenile growth stages and closely resemble *Mesogondolella siciliensis* (Kozur). Mei and Henderson (2002) emphasized that *M. lamberti* has parallel margins in the middle to dorsal part of the platform and a blunt dorsal end, but this is not obvious in juveniles. Mei and Henderson (2002) observed that *M. siciliensis* has wider spacing in the dorsal denticles compared to the ventral denticles. Referring to their illustrations, the wider-spaced dorsal denticles seem to be a feature that distinguishes *M. siciliensis* from *M. lamberti* even in juveniles. The present specimens also resemble *Mesogondolella idahoensis* (Youngquist, Hawley and Miller), which has a much higher cusp even in juveniles (e.g., Igo, 1981). *Jinogondoella aserrata* (Clark and Behnken) is similar, but has a thinner cusp in juveniles (see Plate 6 Fig. 1-4 of Wardlaw, 2015). *Mesogondolella gujioensis* (Igo) has lower denticles.

Genus ***Pseudohindeodus*** Gullo and Kozur, 1992
Type species ***Pseudohindeodus ramovsi***
Gullo and Kozur, 1992

***Pseudohindeodus* sp.** (Fig. 8q)
Remarks: This specimen is a broken scaphate element with a thin cup bearing a ridge parallel to its outline. Its form is similar to *Hindeodus*, but the presence of the ridge places it in a distinct genus (Gullo and Kozur, 1992; Wardlaw, 2000).

Radiolarians (by Tsuyoshi Ito)

Order **ALBAILLELLARIA** Deflandre, 1953
Family **FOLLICUCULLIDAE** Ormiston and Babcock, 1979
Genus ***Haplodiacanthus*** Nazarov and Rudenko, 1981
Type species ***Haplodiacanthus anfractus***
Nazarov and Rudenko, 1981

Haplodiacanthus sakmarensis (Kozur, 1981) (Fig. 9a)
Haplodiacanthus* sp. cf. *H. sakmarensis (Kozur, 1981) (Fig. 9b)
Remarks: The specimen is composed of straight medium-sized apical cone, slightly-inflated pseudothorax with large ventral wing and short, curved short pseudoabdomen with three segmentations. These characteristics are closely similar with the species (Kozur, 1981).

Genus ***Curvalbaillella*** Kozur and Mostler, 1989
Type species ***Pseudoalbaillella u-forma***
Holdsworth and Jones, 1980

Curvalbaillella chilensis (Ling and Forsythe, 1987) (Figs. 9d-g)
Remarks: The specimen is composed of a small apical cone, uninflated pseudothorax with small wings and long curved pseudoabdomen with no segmentation. These characters are characteristic of the species (Ling and Forsythe, 1987).

Curvalbaillella* sp. cf. *C. elegans (Ishiga and Imoto, 1980) (Figs. 9j, k)
Remarks: The specimen is composed of a small apical cone, uninflated pseudothorax and long pseudoabdomen. The pseudoabdomen is slightly curved. Wing and segmentation cannot be observed. These characteristics are closely similar with the species (Ishiga and Imoto, 1980). Because the preservation is poor, these specimens are identified as *C. elegans* with cf.

ACKNOWLEDGEMENTS

The authors thank members of the Geological Sample Preparation Group of the Geoinformation Service Center, GSJ for preparing thin sections for this study and K. Yoshizawa for helping with the illustrations. The authors are grateful to Manuel Rigo and an anonymous reviewer for their comments that improved the manuscript, and to editor Marco Chiari for handling the manuscript.

REFERENCES

Barrick J.E., Hogancamp N.J. and Rosscoe S.J., 2023. Evolutionary patterns in Late Pennsylvanian conodonts. Geol. Soc. London, Spec. Publ., 535: 383-408. https://doi.org/10.1144/sp535-2022-139.

Barrick J.E., Lambert L.L., Heckel P.H., Rosscoe S.J. and Boardman D.R., 2013. Midcontinent Pennsylvanian conodont zonation. Stratigraphy, 10: 55-72.

Beauchamp B., González D.C., Henderson C.M., Baranova D.V., Wang H. and Pelleter E., 2022a. Late Pennsylvanian-Early Permian tectonically driven stratigraphic sequences and carbonate sedimentation along Northern Margin of Sverdrup Basin (Otto Fiord Depression, Arctic Canada). SEPM Spec. Publ., 113: 226-254. https://doi.org/10.2110/sepmsp.113.12

Beauchamp B., Henderson C.M., Dehari E., von Bassenheim D.W., Elliot S. and González D.C., 2022b. Carbonate sedimentology and conodont biostratigraphy of Late Pennsylvanian-Early Permian stratigraphic sequences, Carlin Canyon, Nevada: New insights into the tectonic and oceanographic significance of an iconic succession of the Basin and Range. SEPM Spec. Publ., 113: 34-71. https://doi.org/10.2110/sepmsp.113.14

Bender K.P., 1980. Lower and Middle Pennsylvanian conodonts from the Canadian Arctic Archipelgo, Geol. Surv. Canada Paper, 79-15, Geological Survey of Canada, Ottawa, pp. 29.

Boardman II D.R., Wardlaw B.R. and Nestell M.K., 2009. Stratigraphy and conodont biostratigraphy of the uppermost Carboniferous and Lower Permian from the North American Midcontinent [also on CD], Kansas Geol. Surv. Bull. 255, Kansas Geological Survey, Lawrence, pp. 42.

Chernykh V.V., 2005. Zonal method in biostratigraphy, zonal conodont scale of the Lower Permian in the Urals. Inst. Geol. Geochem. RAN, Ekaterinburg, pp. 217 (in Russian).

Chernykh V.V., 2006. Lower Permian conodonts in the Urals. Inst. Geol. Geochem., Uralian Branch Russ. Acad. Sci., Ekaterinburg, pp. 130 (in Russian)

Clark D.L. and Behnken F.H., 1971. Conodonts and biostratigraphy of the Permian. Mem. Geol. Soc. Am., 127: 415-439. https://doi.org/10.1130/MEM127-p415

Cohen K.M., Finney S.C., Gibbard P.L. and Fan J.-X., 2013; updated. The ICS International Chronostratigraphic Chart. Episodes, 36: 199-204.

Deflandre G., 1953. Radiolaires fossiles. In: P.P. Grassé (Ed.), Traité de Zoologie. Masson, Paris, 389-436.

Dunn D.L., 1970. Middle Carboniferous conodonts from western United States and phylogeny of the platform group. J. Paleont., 44: 312-342.

Ehiro M., Komori K., Tsuchiya N., Kawamura T., Yoshida H. and Oishi M., 2010. Carboniferous ammonoids and corals from seamount limestone in an accretionary complex within the North Kitakami Belt, Northeast Japan. J. Geol. Soc. Japan, 116: 219-228. https://doi.org/10.5575/geosoc.116.219

Ehiro M., Yamakita S., Takahashi S. and Suzuki N., 2008. Jurassic accretionary complexes of the North Kitakami Belt in the Akka-Kuji area. J. Geol. Soc. Japan, 114: 121-139. (in Japanese)

Geological Survey of Japan, AIST, 2020. Seamless digital geological map of Japan 1: 200,000. Geol. Surv. Japan, AIST. https://gbank.gsj.jp/seamless/v2full/ (Accessed: 2021-10-08)

Gullo M. and Kozur H., 1992. Conodonts from the pelagic deepwaer Permian of central Western Sicily (Italy). Neues Jahrb. Geol. Palaont., Abh., 184: 203-234.

Gunnell F.H., 1931. Conodonts from the Fort Scott Limestone of Missouri. J. Paleont., 5: 244-252.

Gunnell F.H., 1933. Conodonts and fish remains from the Cherokee, Kansas City, and Wabaunsee groups of Missouri and Kansas. J. Paleontol., 7: 261-297.

Hamano K., Iwata K., Kawamura M. and Kitakami Paleozoic Research Group, 2002. Late Devonian conodont age of red chert intercalated in greenstones of the Hayachine Belt, Northeast Japan. J. Geol. Soc. Japan, 108: 114-122. (in Japanese)

Harris R.W. and Hollingsworth R.V., 1933. New Pennsylvanian conodonts from Oklahoma. Am. J. Sci., 5: 193-204.

Henderson C.M., 2018. Permian conodont biostratigraphy. Geol. Soc. Spec. Publ. 450: 119-142. https://doi.org/10.1144/SP450.9

Holdsworth B.K. and Jones D.L., 1980. Preliminary radiolarian zonation for late Devonian through Permian time. Geology, 8: 281-285.

Hu K., Hogancamp N.J., Lambert L.L., Qi Y. and Chen J., 2020a. Evolution of the conodont *Diplognathodus ellesmerensis* from *D. benderi* sp. nov. at the Bashkirian–Moscovian (lower-middle Pennsylvanian) boundary in South China. Pap. Palaeont., 6: 627-649. https://doi.org/10.1002/spp2.1309

Hu K., Qi Y., Qi W. and Wang Q., 2020b. Carboniferous conodont zonation of China. Newslett. Stratigr., 53: 141-190. https://doi.org/10.1127/nos/2019/0498

Igo H., 1981. Permian conodont biostratigraphy of Japan. Palaeont. Soc. Japan, Spec. Pap., 24: 1-51.

Igo H. and Kobayashi F., 1974. Carboniferous conodonts from the Itsukaichi District, Tokyo, Japan. Trans. Proc. Palaeont. Soc. Japan. New Ser., 96: 411-426. https://doi.org/10.14825/prpsj1951.1974.96_411

Imoto N., Kusunoki T. and Obara M., 1997. Geology Part. In: Research Center for Cultural Property in the Osaka Prefectural Government (Ed.), A comprehensive research on cultural and other properties associated with the developmental project of the Aigawa River: Interim Report. Nature, History and Culture of the Construction Area of the Aigawa Dam. Osaka, pp. 57-106.*

Ishida K., 1979. Studies of the South Zone of the Chichibu Belt in Shikoku, Part 2-Stratigraphy and structure around Nagayasuguchi Dam, Tokushima Prefecture-. J. Sci. Univ. Tokushima, 12: 61-92. (in Japanese with English abstract)

Ishida K., 1985. Pre-Cretaceous sediments in the southern North Zone of the Chichibu Belt in Tokushima Prefecture, Shikoku. J. Geol. Soc. Japan, 91: 553-567. https://doi.org/10.5575/geosoc.91.553 (in Japanese with English abstract)

Ishiga H., 1982. Late Carboniferous and Early Permian radiolarians from the Tamba Belt, Southwest Japan. Earth Sci. J. Assoc. Geol. Collab. Japan, 36: 333-339.

Ishiga H. and Imoto N., 1980. Some Permian radiolarians in the Tamba District, Southwest Japan. Earth Sci., J. Ass.Geol. Collabor. Japan, 34 (6): 333-345.

Isozaki, Y. and Maruyama, S., 1991. Studies on Orogeny based on Plate Tectonics in Japan and New Geotectonic Subdivision of the Japanese Islands. J. Geogr. (Chigaku Zasshi), 100: 697-761. https://doi.org/10.5026/jgeography.100.5_697

Isozaki Y., Maruyama S., Aoki K., Nakama T., Miyashita A. and Otoh S., 2010. Geotectonic subdivision of the Japanese Islands revisited: categorization and definition of elements and boundaries of Pacific-type (Miyashiro-type) orogen-. Chigaku Zasshi (J. Geogr.), 119: 999-1053. https://doi.org/10.5026/jgeography.119.235 (in Japanese with English abstract)

Isozaki Y., Maruyama S. and Furuoka F., 1990. Accreted oceanic materials in Japan. Tectonophysics, 181: 179-205. https://doi.org/10.1016/0040-1951(90)90016-2

Ito T. and Matsuoka A., 2018. Lithology and radiolarian age of the Ryokami-yama Chert Formation in eastern Mt. Ryokami: Possible décollement zone in Permian pelagic sequence in mid-Mesozoic accretionary complexes of Southwest Japan. Isl. Arc, 27: e12273. https://doi.org/10.1111/iar.12273

Iwate Prefecture, 1954. Geological Map of Iwate Prefecture, 1:10,000. Nagai Co., Ltd., Chiba*

Kawamura T., Uchino T., Kawamura M., Yoshida K., Nakagawa M. and Nagata H., 2013. Geology of the Hayachinesan District. Quadrang. Ser. 150,000, Geol. Surv. Japan, AIST, 101p. (in Japanese with English abstract, 4p)

Koike T., 2016. Multielement Conodont apparatuses of the Ellisonidae from Japan. Paleont. Res., 20: 161-175. https://doi.org/10.2517/2016pr007

Kojima S., Hayasaka Y., Hiroi Y., Matsuoka A., Sano H., Sugamori Y., Suzuki N., Takemura S., Tsujimori T. and Uchino T., 2016. 2b Pre-Cretaceous accretionary complexes. In: T. Moreno, S. Wallis, T .Kojima and W.Gibbons (Eds.), The Geology of Japan. Geol. Soc. London, pp. 61-100.

Kozur H.W., 1975. Beiträge zur Conodontenfauna des Perm. Geol. Mitteilungen Innsbruck, 5: 1-41. (in German with English summary)

Kozur H., 1981. Albaillellidae (Radiolaria) aus dem Unterperm des Vorurals. Geologisch Paläontologische Mitteil. Innsbruck, 10 (8): 263-274.

Kozur H.W., 1989. The taxonomy of the gondolellid conodonts in the Permian and Triassic. 1st Int. Senckenb. Conf. 5th Eur. conodont Symp. (ECOS V); Contrib. III, Pap. Ordovician to Triassic conodonts, 117: 409-469.

* English translation from the original written in Japanese.

Kozur H. and Mostler H., 1989. Radiolarien und schwammskleren aus dem Unterperm des Vorurals. Geol. Paläont. Mitteil. Innsbruck, Sonderb., 2, 147-275. (in German)

Kurimoto C., Matsuura H. and Yoshikawa T., 1993. Geology of the Sasayama district. With Geological Sheet Map at 1: 50,000, Geol. Surv. Japan, 93p (in Japanese with English abstract 5p)

Kusunoki T., Ohara M. and Musashino M., 2004. Carboniferous-Permian microbiostratigraphy in chert sequence from the southeastern part of the Tamba Belt, Shizugawa district, Uji City (Outline note) (in Japanese with English abstract). Earth Sci. (Chikyu Kagaku), 58: 37-54.

Lambert L.L., Heckel P.H. and Barrick J.E., 2003. *Swadelina* new genus (Pennsylvanian conodonta), a taxon with potential chronostratigraphic significance. Micropaleontology, 49: 151-158. https://doi.org/10.2113/49.2.151

Lambert L.L., Wardlaw B.R. and Henderson C.M., 2007. Mesogondolella and Jinogondolella (Conodonta): Multielement definition of the taxa that bracket the basal Guadalupian (Middle Permian Series) GSSP. Palaeoworld, 16: 208-221. https://doi.org/10.1016/j.palwor.2007.05.017

Lane H.R., 1967. Uppermost Mississippian and Lower Pennsylvanian conodonts from the type Morrowian Region, Arkansas. J. Paleontol., 41: 920-942.

Lane H.R. and Straka J.J., 1974. Late Mississippian and Early Pennsylvanian conodonts, Arkansas and Oklahoma. Geol. Soc. Am. Boulder, 144p.

Ling H.Y. and Forsythe R.D., 1987. Late Paleozoic Pseudoalbaillellid radiolarians from southernmost Chile and their geologic significance. In: G.D. Mckenzie (Ed.), Gondwana Six; structure, tectonics, and geophysics. Am. Geophys. Union, Geophys. Monogr.. 40): 253-260. https://doi.org/10.1029/GM040p0221

Matsuoka A., 1987. Radiolarian age of the Shiriya Group in Aomori Prefecture, northeast Japan. Fossils, 42: 7-13. (in japanese with English abstract)

Matsuoka A., 1988. Discovery of Early Jurassic radiolarians from the North Kitakami Belt (s. s.), northeast Japan. Earth Sci. (Chikyu Kagaku), 42: 104-106.

Matsuoka A. and Oji T., 1990. Middle Jurassic radiolarian fossils from the Magisawa Formation in the Taro Belt, North Kitakami Mountains. J. Geol. Soc. Japan, 96: 239-241. (in Japanese)

Mei S. and Henderson C.M., 2001. Evolution of Permian conodont provincialism and its significance in global correlation and paleoclimate implication. Palaeo. Palaeo. Palaeo., 170: 237-260. https://doi.org/10.1016/S0031-0182(01)00258-9

Mei S. and Henderson C.M., 2002. Conodont definition of the Kungurian (Cisuralian) and Roadian (Guadalupian) boundary. In: L.V Hills, C.M. Henderson and E.W. Bamber (Eds.), The Carboniferous and Permian of the World: 14th ICCP Proceed. Can. Soc. Petrol. Geologists, Calgary, pp. 529-551.

Merrill G.K., 1973. Pennsylvanian nonplatform conodont genera I: Spathognathodus. J. Paleont., 47: 289-314.

Metcalfe I., 2023. Lower Permian (Late Kungurian) conodonts from the Sibumasu Terrane, Malaysia: Paleoecological, paleobiogeographical and tectonic implications. Geol. Mag., 197: 1-16. https://doi.org/10.1017/S0016756823000328

Minoura K. and Tsushima M., 1984. Geology of the Omoto district in the eastern margin of the North Kitakami Massif. Sci. reports Hirosaki Univ., 31: 93-107.

Miyachi Y., KusunokiT., MusashinoM., TainoshoY. and ImotoN., 2005. Geology of the Kyoto-Seinambu district. Quadrangle Series, 1:50,000, Geo. Surv. Japan, AIST, 90 pp (in Japanese with English abstract 4p).

Müller K.J., 1956. Triassic conodonts from Nevada. J. Paleontol., 30: 818-830.

Murray F.N. and Chronic J., 1965. Pennsylvanian conodonts and other fossils from isoluble residues of the Minturn Formation (Desmoinesian), Colorado. J. Paleontol., 39: 594-610.

Muto S., Ito T. and Murayama M., 2023a. Geology and accretionary age of the Otori Unit, North Kitakami Belt. Bull. Geol. Surv. Japan, 74: 1-40.

Muto S., Takahashi S. and Murayama M., 2023b. Conodont biostratigraphy of a Carboniferous-Permian boundary section in siliceous successions of pelagic Panthalassa revealed by X-ray computed microtomography. Front. Earth Sci., 11: 1-19. https://doi.org/10.3389/feart.2023.1162023

Muto S., Takahashi S. and Yamakita S., 2023c. Elevated sedimentation of clastic matter in pelagic Panthalassa during the early Olenekian. Isl. Arc, 32: e12485.

Nakae S., 2000. Regional correlation of the Jurassic accretionary complex in the Inner Zone of Southwest Japan. Mem. Geol. Soc. Japan, 55: 73-98. (in Japanese with English abstract)

Nakae S. and Kamada K., 2003. Late Jurassic radiolarians from the Rikuchu-Seki district in the North Kitakami Belt, Northeast Japan. J. Geol. Soc. Japan, 109: 722-725. (in Japanese with English abstract)

Nazarov B.B. and Rudenko V.S., 1981. Some bilaterally symmetric late Paleozoic radiolarians of the South Urals, Vopr. Micropal., 24: 129-139.

Nemyrovska T.I., 1999. Bashkirian conodonts of the Donets Basin, Ukraine. Scr. Geol., 25: 1-115.

Nemyrovska T.I., 2017. Late Mississippian-Middle Pennsylvanian conodont zonation of Ukraine. Stratigraphy, 14: 299-318. https://doi.org/10.29041/strat.14.1-4.299-318

Onuki Y., 1981. Part 1. The Kitakami Mountains. In: Hase Chishitsu Chosa Jimusho (Ed.), Explanation of the Geological Map of the Kitakami River Area, Kitakami Mountains, at the Scale of 1: 20,000. Hase Chishitsu Chosa Jimusho, Sendai, pp. 3-223. (in Japanese)

Orchard M.J. and Forster, P.J.L., 1988. Permian conodont biostratigraphy of the Harper Ranch Beds, near Kamloops, south-central British Colubmia. Geol. Surv. Canada, Pap., 88-8: 1-27. https://doi.org/https://doi.org/10.4095/126428

Osaka M., Aoki S., Uchino T. and Fukuyama M., 2023. Constraint on the spatial distribution of the Early and Middle Jurassic units within the Nakatsugawa Complex of the North Kitakami Belt by detrital zircon U - Pb dating. Bull. Geol. Surv. Japan, 74: 155-166.

Ormiston A.R and Babcock L., 1979. *Follicucullus*, new radiolarian genus from the Guadalupian (Permian) Lamar limestone of the Delaware Basin. J. Paleont., 53: 328-334.

Rexroad C.B., 1957. Conodonts from the Chester Series in the type area of Southwestern Illinois. Div. State Geol. Surv. Rep. Investig., 199: 1-43. https://doi.org/10.1007/978-3-642-41714-6_70729

Rexroad C.B. and Furnish W.M., 1964. Conodonts from the Pella Formation (Mississippian), south-central Iowa. J. Paleontol. 38: 667-676.

Ritter S.M., 1995. Upper Missourian-Lower Wolfcampian (Upper Kasimovian-Lower Asselian) conodont biostratigraphy of the midcontinent, U.S.A. J. Paleont., 69: 1139-1154. https://doi.org/10.1017/S0022336000038129

Salvador A., 2013. International Stratigraphic Guide. Geological Society of America, Boulder. Boulder, pp. 214. https://doi.org/10.1130/9780813774022

Sun Y.D., Liu X.T., Yan J.X., Li B., Chen B., Bond D.P.G., Joachimski M.M., Wignall P.B., Wang X. and Lai X.L., 2017. Permian (Artinskian to Wuchapingian) conodont biostratigraphy in the Tieqiao section, Laibin area, South China. Palaeo. Palaeo. Palaeo.., 465: 42-63. https://doi.org/10.1016/j.palaeo.2016.10.013

Suzuki N. and Ogane K., 2004. Paleoceanographic affinities of radiolarian faunas in late Aalenian time (Middle Jurassic) recorded in the Jurassic accretionary complex of Japan. J. Asian Earth Sci., 23: 343-357. https://doi.org/10.1016/S1367-9120(03)00113-5

Suzuki N., Ehiro M., Yoshihara K., Kimura Y., Kawashima G., Yoshimoto H. and Nogi T., 2007a. Geology of the Kuzumaki-Kamaishi Subbelt of the North Kitakami Belt (a Jurassic accretionary complex), Northeast Japan: Case study of the Kawai-Yamada area, eastern Iwate Prefecture. Bull.Tohoku Univ.Museum, 6: 103-174.

Suzuki N., Yamakita S., Takahashi S. and Ehiro M., 2007b. Middle Jurassic radiolarians from carbonate manganese nodules in the Otori Formation in the eastern part of the Kuzumaki-Kamaishi Subbelt, the North Kitakami Belt, Northeast Japan. J. Geol. Soc. Japan, 113: 274-277. https://doi.org/10.5575/geosoc.113.274 (in Japanese with English abstract).

Sweet W.C., 1977. Hindeodus, In: W. Ziegler (Ed.), Catalogue of Conodonts, Vol. 3. Schweizerbartsche Verlagsbuchhandlung, Stuttgart, pp. 203-224.

Uchino T., 2017. Late Triassic U-Pb-zircon age from tuffaceous mudstone in the Kadoma Complex, North Kitakami Belt, Northeast Japan. J. Geol. Soc. Japan, 123: 977-982. https://doi.org/10.5575/geosoc.2017.0024 (in Japanese with English abstract).

Uchino T., 2018a. Detrital zircon U–Pb age of the Jurassic accretionary complex in the western area of Lake Towada located between Akita and Aomori prefectures, Northeast Japan. Bull. Geol. Surv. Japan, 69: 37-46. (in Japanese with English abstract)

Uchino T., 2018b. Detrital zircon U-Pb age of sandstone within the Jurassic accretionary complex in the Omori area, northeastern Shimokita Peninsula, Northeast Japan. Bull. Geol. Surv. Japan, 69: 125-133. (in Japanese with English abstract)

Uchino T., 2019. Detrital zircon U-Pb ages of sandstone within the Jurassic accretionary complex in the North Kitakami Belt of the Sotoyama District, Iwate Prefecture. Bull. Geol. Surv. Japan, 70: 357-372. (in Japanese with English abstract)

Uchino T., 2021a. Middle Jurassic zircon age from sandstone within the accretionary complex in the North Kitakami Belt, Kamatsuda area in Iwaizumi Town, Iwate Prefecture, Northeast Japan: Verifying the age of the accretionary complex containing the Okawa Sample. Bull. Geol. Surv. Japan, 72: 99-107. (in Japanese with English abstract)

Uchino T., 2021b. Geochemical features and origin of basalt within the Jurassic accretionary complex in the southwestern margin of the North Kitakami Belt, Northeast Japan. Bull. Geol. Surv. Japan, 72: 109-118.

Uchino T., 2024. Chapter 8, Early to Middle Jurassic accretionary complex., in: Geology of the Sotoyama District. Quadrangle Series, 1:50,000, Geol. Surv. Japan, AIST. Tsukuba, pp. 53-67. (in Japanese)

Uchino T. and Suzuki N., 2020. Late Jurassic radiolarians from mudstone near the U-Pb-dated sandstone of the North Kitakami Belt in the northeastern Shimokita Peninsula, Tohoku, Japan. Bull. Geol. Surv. Japan, 71: 313-330. https://doi.org/10.9795/bullgsj.71.313

Uchino T. and Suzuki N., 2021. Mesozoic radiolarian fossils from mudstone within the accretionary complex in the southwestern margin of the North Kitakami Belt, eastern Morioka, Iwate Prefecture, Northeast Japan. Bull. Geol. Surv. Japan, 72: 119-127. https://doi.org/10.9795/bullgsj.72.119 (in Japanese with English abstract)

Uchino T., Kawamura M. and Kawamura T., 2008. Lithology of the Nedamo Terrane, an Early Carboniferous accretionary complex, and its southern boundary with the South Kitakami Terrane (in Japanese). J. Geol. Soc. Japan 114, Suppl: 141-157.

Ueda H., Kimura S., Saito T., Takano Y., Iizuka N. and Orihashi Y., 2018. Material recycling in a sediment-starved trench recorded in the Early Cretaceous Shiriya accretionary complex, Northeast Japan. Isl. Arc, 27: 1-20. https://doi.org/10.1111/iar.12272

Ueda H., Mori M. and Sato I., 2009. Early Jurassic radiolarian fossils from mudstone within an accretionary complex south of Hirosaki City, Aomori Prefecture, Japan. J. Geol. Soc. Japan, 115: 610-613. (in Japanese with English abstract)

von Bitter P.H. and Merrill G.K., 1983. Late Palaeozoic species of *Ellisonia* (Conodontophorida) Evolutionary and palaeoecological significance. R. Ontario Museum Life Sci. Contrib., 136: 1-57.

Wakita K. and Metcalfe I., 2005. Ocean plate stratigraphy in East and Southeast Asia. J. Asian Earth Sci., 24: 679-702. https://doi.org/10.1016/j.jseaes.2004.04.004

Wakita K., Takeuchi K., MizunoK., Komatsubara T., Nakano S., Takemura K. and Taguchi Y., 2013. Geology of the Kyoto-Tonambu District. Quadrangle Series, 1:50,000, Geol. Surv. Japan, AIST, 124 pp. (in Japanese with English abstract, 3p.)

Wang Z. and Qi Y., 2003. Upper Carboniferous (Pennsylvanian) conodonts from South Guizhou of China. Riv. It. Paleont. Stratigr., 109: 379-397.

Wardlaw B.R., 2000. Guadalupian conodont biostratigraphy of the Glass and Del Norte Mountains.In: B.R. Wardlaw, R.E. Grant and D.M. Rohr (Eds.), The Guadalupian Symp. Smithsonian Contrib. Earth Sci., 22. Smithsonian Instit. Press, Washington pp. 37-87.

Wardlaw B.R., 2015. Gondolellid conodonts and depositional setting of the Phosphoria Formation. Micropaleontology, 61: 335-368.

Wardlaw B.R. and Nestell M.K., 2015. Conodont faunas from a complete basinal succession of the upper part of the Wordian (Middle Permian, Guadalupian, West Texas). Micropaleontology, 61: 257-292.

Xiao, Y.F., Suzuki N. and He W.H., 2018. Low-latitudinal standard Permian radiolarian biostratigraphy for multiple purposes with Unitary Association, Graphic Correlation, and Bayesian inference methods. Earth-Sci. Rev., 179: 168-206.

Yoshida K. and Matsuoka A., 2003. Pile-nappe structure of the Ryokami-yama chert unit in the Chichibu composite terrane of the Kanto Mountains, central Japan. J. Geol. Soc. Japan, 109: 324-335. (in Japanese with English abstract)

Yoshida T., Ozawa A., Katada M. and Nakai J., 1984. Geological Map of Japan 1:200,000, Morioka.

Yoshihara K., Suzuki N. and Ehiro M., 2002. Middle Jurassic radiolarian-bearing manganese nodules from the Kuzumaki-Kamaishi Belt in the Northern Kitakami Massif and its significance. J. Geol. Soc. Japan, 108: 536-539.

Ziegler A.M., Hulver M.L. and Rowley D.B., 1997. Permian world topography and climate In: I.P. Martini (Ed.), Late Glacial and Postglacial environmental changes-Quaternary, Carboniferous, Permian and Proterozoic. Oxford Univ. Press, New York, pp. 111-146.

Received, October 6, 2023
Accepted, July 11, 2024